Modeling of frictional contact interaction of spherical particles

***R. Balevičius*[1] *and Z. Mròz*[2]**
[1] *Vilnius Gediminas Technical University, Vilnius, Lithuania*
[2] *Institute of Fundamental Technological Research, Warsaw, Poland*

1. Introduction

In the frictional contact interaction of two spherical grains, there are two fundamental deformation regimes, namely, the partial slip and sliding, developed consecutively in the progressive motion [1]. For the reciprocal motion, these two regimes develop consecutively during each grain motion reversal. However, for a specified trajectory of the sphere centre, when both normal and tangential tractions vary along with the variation of the contact zone size and its orientation, there is an instantaneous development of sliding regime without initial evolution of the slip mode [2]. For oblique loading of two grains the previous analysis was addressed to growth of slip regime from the contact zone boundary into the sticking zone in the central part of contact. The slip memory rules in terms of the loading surfaces in the $\underset{\sim}{\mathbf{T}} - N$ space (where $\underset{\sim}{\mathbf{T}}$ is the tangential load vector and N is the normal load to the contact plane) have also been developed [3], [4], in order to resolve this complicated phenomenon.

In the present work, the problem of multiple contact interaction with a simultaneous contact separation/activation of the sphere motion over the regularly packed granular bed is considered. The slip, sliding or their mixed modes are analytically studied, while their evolution presented in terms of loading surfaces.

2. Analysis of the sphere contact response with the granular bed

Let us consider the contact interaction of an elastic sphere of radius R_2 with a bed of spheres of radius R_1 fixed on a rigid substrate (Figure 1a).

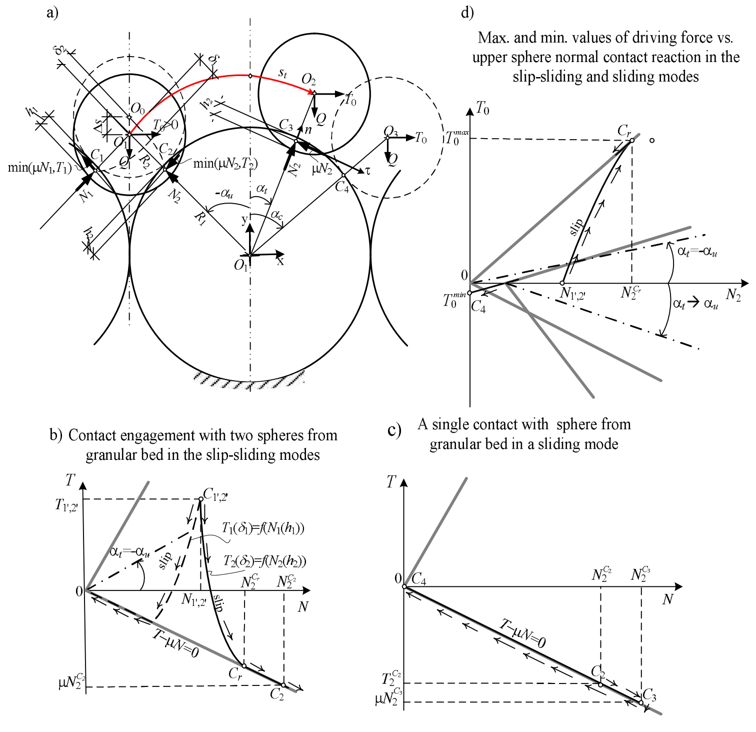

Figure 1 Sphere contact interaction with the regularly packed granular bed: evolution of contact tractions

Initially, the sphere is placed to touch two bottom spheres at the point O_0 (Figure 1a). Next, the vertical load Q is statically applied and held constant. The sphere motion is induced by the horizontal force T_0. The sphere center initial displacement Δs, its motion path s_t, evolution of contact tractions and of overlaps h_1, h_2, etc. should be specified from the analysis.

For the large radii of upper spheres, such that $R_2 > \xi_c R_1$ (where $\xi_c = \sin^{-1}\phi_u - 1$, $\tan\phi_u = \mu/2(1+\nu/2)$, ν is the Poison ratio), the application of force Q yields the contact engagement in a slip mode. For example, for $\mu = 0.5$, $\nu = 0.3$, the vertical slip response can be obtained, when $R_2 > 3.6R_1$. Otherwise, the sliding mode is generated by load Q.

After application of Q, the normal and tangential tractions $N_{1',2'}$ and $T_{1',2'}$ are generated (Figure 1b). Next, a gradual growth of driving force T_0 deforms the upper sphere and produces the increase in the overlap h_1 and decrease in the overlap h_2. The deformation process starts in a slip mode with the evolution of tangential slip displacements δ_1, δ_2, generated at the sphere center. The *N-T* loading surface evolution in slip-sliding mode is shown in Figure 1b. The normal contact force N_1 at the left bottom sphere contact decreases non-linearly vs. the decreasing tangential force T_1, which tends to the limit locus. When the force path $T_1(N_1)$ touches the limit friction locus, the sliding mode proceeds on the bottom left sphere and the unloading process for N_1 continues within this mode until the contact separation at the left contact occurs, when N_1=0. However, for the right bottom sphere, the force path of $T_2(N_2)$ monotonically grows up and finally attains the Coulomb limit locus (denoted by point C_r in Figure 1b). When the slip regime terminates at the bottom right sphere, the maximal value of the driving force is reached (Figure 1d). Next, the sliding process yields the variation in the orientation of contact plane and diminishing values of force T_0. Depending on the upper sphere radius and friction coefficient the minimal negative value of T_0 could also be reached (Figure 1d). When N_1=0, the single contact sliding mode develops on the right bottom sphere (Figure 1c). In this case, the $T_2(N_2)$ function monotonically decreases to zero at the point C_4 following the sliding friction rule (Figure 1c). When $T_2(N_2)\rightarrow 0$, the upper sphere activates the contact with the next bottom sphere 3 from the granular bed. In this case, the contact activation is non-symmetric, since $N_2 \neq N_3$. In this case, the $T_3(N_3)$ function starts with some initial portion of force N_2 caused by minimal overlap, which should be selected to avoid the singularity in the incremental solution.

3. Concluding remarks

The evaluation of contact tractions during sphere interaction with the regularly packed granular bed has been presented. It was demonstrated that the contact activation/separation processes develops in the combined or mixed slip-sliding modes, essentially affecting the contact traction distributions. The results presented can be applied in the experimental testing of frictional response of contacting bodies. They are also relevant for the ongoing development of the discrete element method.

4. References

[1] R.D. Mindlin and H. Deresiewicz, (1953). Elastic spheres in contact under varying oblique forces, *Journal of Applied Mechanics*, **20**, 327-344.

[2] R. Balevičius, Z. Mróz (2013). A finite sliding model of two identical spheres under displacement and force control—part I: static analysis, *Acta Mechanica*, **224**(8), 1659–1684.

[3] R. Dobry, T.-T. Ng, E. Petrakis and A. Seridi (1991). General model for contact law between two rough spheres, *Journal of Engineering Mechanics*, **117**, 1365-1381.

[4] A. Jarzębowski and Z. Mróz (1994). On slip and memory rules in elastic, friction contact problems, *Acta Mechanica*, **102**, 199-216.